

## Enhanced ionization of an inner orbital of $I_2$ by strong laser fields

H. Chen, V. Tagliamonti, and G. N. Gibson

*Department of Physics, University of Connecticut, Storrs, Connecticut 06269, USA*

(Received 3 October 2012; published 28 November 2012)

Using pump-probe spectroscopy, strong-field enhanced-ionization is found in an inner orbital of  $I_2$ . A wave packet is launched in the  $B$  state of  $I_2$ , whose valence orbitals are  $\sigma_g^2\pi_u^4\pi_g^3\sigma_u^1$ , and singly ionized to the  $I + I^+$  dissociation channel. The ionization signal peaks at two different internuclear separations:  $\sim 7.3$  and  $\sim 8.7$  a.u. The latter shows enhanced ionization of the  $\sigma_u$  state which has been studied before with the  $I_2^+$  signal. However, the peak at smaller  $R$  corresponds to enhanced ionization of the  $\sigma_g$  state. The peak at  $\sim 8.7$  a.u. in the dissociating channel reveals that there could be strong mixing of different molecular orbitals when the two iodine atoms are pulled apart.

DOI: [10.1103/PhysRevA.86.051403](https://doi.org/10.1103/PhysRevA.86.051403)

PACS number(s): 33.80.Rv, 32.80.Rm, 42.50.Hz

For diatomic molecules driven by intense laser fields linearly polarized along the molecular axis, their tunneling ionization rate increases with the internuclear separation  $R$  and peaks at a critical separation  $R_c$ . This very general phenomenon, known as enhanced ionization (EI), has been found in many experiments [1–5].

Theoretically, EI has been rigorously studied in a few relatively simple cases: one-electron molecules, such as  $H_2^+$ , and the two-electron molecule  $H_2$ . For a one-electron system, the mechanism of EI is electron localization (EL) [6,7] and charge-resonance-enhanced ionization (CREI) [8,9]. It is predicted that  $R_c \sim 3/I_p$  from EL and  $R_c \sim 4/I_p$  from CREI, where  $I_p$  is the atomic ionization potential. Furthermore, EI is highly dependent on molecular symmetry and  $R_c$  occurs only for  $\sigma$  states, not for  $\pi$  or  $\delta$  [10]. For the two-electron system, it is believed that the charge transfer from the covalent state to the ionic state is the crucial step and the ionic state works as the ionization doorway state [11–14].

In our previous work [5], we investigated EI in the  $B$  state ( $\sigma_g^2\pi_u^4\pi_g^3\sigma_u^1$ ) of  $I_2$  by using a pump-probe technique. The pump pulse promoted one electron from the highest occupied molecular orbital (HOMO)  $\pi_g$  state to the lowest unoccupied molecular orbital (LUMO)  $\sigma_u$  state, and the probe pulse removed the electron in the  $\sigma_u$  state, leaving the molecular ions in the deeply bound  $I_2^+ X^2\Pi_{3/2g}$  state. The vibrational wave packet (VWP) motion in the  $B$  state provided a large range of  $R$ , and  $R_c$  was found to be at  $\sim 8.7$  a.u. More recently [15], we produced a VWP moving between 4.4 and 6.2 a.u. in the ground electronic state ( $\sigma_g^2\pi_u^4\pi_g^4\sigma_u^0$ ) of  $I_2$ , and discussed the  $R$ -dependent single ionization of different orbitals. We found that the HOMO  $-2\sigma_g$  orbital showed a strong  $R$  dependence, while the HOMO  $\pi_g$  and HOMO  $-1\pi_u$  orbitals did not, and the HOMO  $-2\sigma_g$  orbital provided the dominant single-ionization pathway. We even predicted that the  $\sigma_g$  orbital would also show an  $R_c$  if the VWP moved to a sufficiently large  $R$ .

In this work, using the pump-probe technique described in Ref. [5], we obtain a large range of VWP motion in the  $B$  state of  $I_2$  over which the  $R$ -dependent single ionization of the HOMO  $-2\sigma_g$  orbital is observed by analyzing the final state of the (1,0) dissociation channel [(1,0) refers to the dissociating channel  $I_2^+ \rightarrow I^+ + I$ ], and we find an  $R_c$  at  $\sim 7.3$  a.u. Furthermore, the HOMO  $-2\sigma_g$  orbital again provides the dominant ionization pathway. However, another peak at

$\sim 8.7$  a.u. in the (1,0) channel reveals that different molecular orbitals might be strongly mixed at large  $R$  since the (1,0) channel shows the ionization feature of the LUMO  $\sigma_u$  orbital [5].

The pump-probe scheme is shown in Fig. 1. A VWP is launched in the  $B$  state by a weak green pump pulse through one-photon resonant excitation, and then singly ionized by a delay-controllable 800 nm probe pulse. With a 513 or 500 nm pump pulse, the VWP reaches  $R \sim 8.72$  a.u. or  $\sim 9.38$  a.u., respectively, and the VWP motion is well understood [5]. Both of the pulses are linearly polarized along the time of flight (TOF) axis. Since the  $X-B$  transition is a parallel transition [16], the molecules excited in the  $B$  state will be aligned with the pump laser polarization with a  $\cos^2(\theta)$  distribution [5] in which the  $\sigma$  orbitals will be preferentially ionized. In the molecular orbital picture, the molecules end up in the  $I_2^+ X^2\Pi_{g3/2}$  state by removing the electron from the LUMO  $\sigma_u$  orbital, but in the (1,0) channel by removing one electron in the HOMO  $-2\sigma_g$  orbital [17].

The experiments are performed with our home-built ultrafast Ti:sapphire laser system and a TOPAS (optical parametric amplifier) system. The ionization signals of  $I_2^+$  and  $I^+$  are recorded with a TOF spectrometer. The ultrafast laser and the TOF spectrometer have been described in Refs. [5,18]. Room-temperature (295 K)  $I_2$  gas is leaked effusively into the chamber with a base pressure of  $2 \times 10^{-9}$  torr. The Ti:sapphire laser produces linearly polarized pulses with a central wavelength of 800 nm, a transform-limited pulse duration of 37 fs, and an output energy of up to 800  $\mu$ J at a repetition rate of 1 kHz. The output beam is split with  $\sim 80\%$  of the energy sent into the TOPAS to generate a pump beam while the rest serves as a probe beam. The pump pulses have a central wavelength of 513 or 500 nm, a duration of 50 fs, and an energy of up to 2  $\mu$ J. The pump and probe beams are focused by a 3-in.-focal-length silver spherical mirror inside the TOF chamber. An aperture is used in the pump beam in order to decrease ionization and also increase the focus spot in the chamber. This creates a more uniform focal volume for the probe beam. The pump-probe delay  $\tau$  is adjusted by a computer-controlled translational stage. In the experiments, the probe pulse just singly ionizes the  $B$  state to avoid double ionization [19].

The ionization signals of the  $I_2^+$  and (1,0) channel as functions of  $\tau$  with different pump wavelengths are shown in Fig. 2. With either wavelength, the  $I_2^+$  signal shows one peak, while the (1,0) channel shows two peaks. The peaks

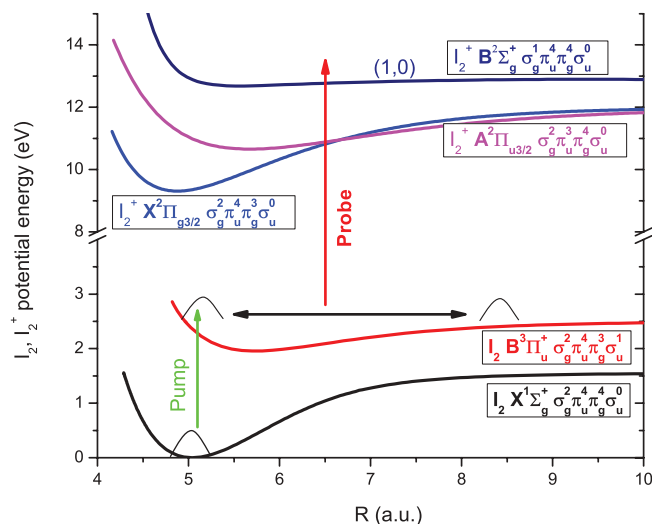


FIG. 1. (Color online) Schematic potential energy curves, showing the physical scenario of the pump-probe experiments.

with 500 nm pump wavelength appear earlier than those with 513 nm, since the 500 nm pump wavelength starts the VWP higher up in the potential curve of the  $B$  state of  $I_2$  and the VWP moves faster. The ionization signals of the  $(1,0)$  channel are much stronger than those of  $I_2^+$  with either wavelength which is consistent with our previous study [15]. The corresponding signal from the  $I_2^+$  or  $(1,0)$  channel with 513 nm is stronger than those with 500 nm, due to the stronger  $X$ - $B$  coupling at 513 nm [20]. There is only one peak in either of the  $I_2^+$  curves, which shows the EI of the LUMO  $\sigma_u$  orbital [5], and there are two peaks in both the  $(1,0)$  channel curves, with the inner one not seen in  $I_2^+$  and the outer one occurring at the same delay as in the  $I_2^+$ .

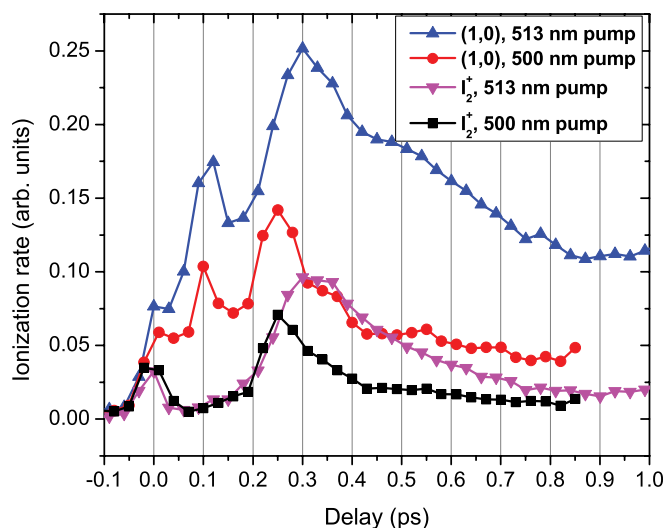


FIG. 2. (Color online) The ionization signals of the  $I_2^+$  and  $(1,0)$  channel as a function of  $\tau$  (background subtracted) with a step size of 0.030 ps with two different pump wavelengths. The delay of 0 ps is the temporal overlap of the pump and probe pulses. In the experiments, the intensities of the pump and probe pulses are estimated to be  $\sim 1.4 \times 10^{11}$  and  $\sim 1.4 \times 10^{13}$  W/cm<sup>2</sup>, respectively, and the  $I_2$  pressure is  $\sim 7.0 \times 10^{-7}$  torr.

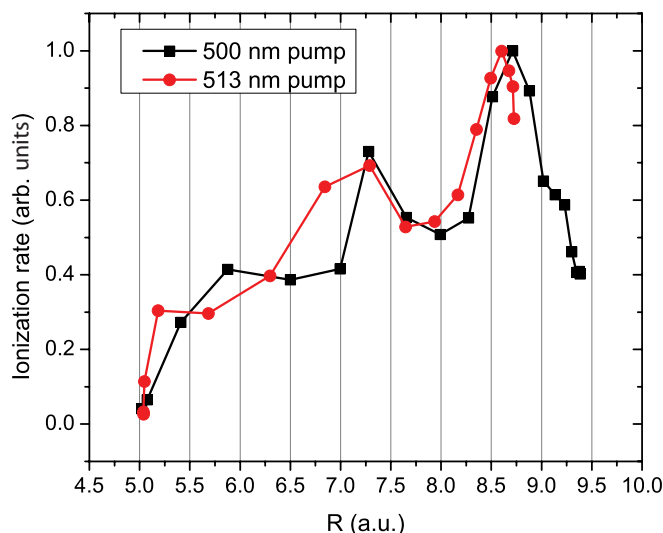


FIG. 3. (Color online) The ionization signal (normalized) of the  $(1,0)$  channel as a function of  $R$  with two different pump wavelengths: 500 and 513 nm. There are two  $R_c$ 's: the inner one at  $\sim 7.3$  a.u. and the outer one at  $\sim 8.7$  a.u. The peaks at  $\sim 5.9$  a.u. (500 nm) and  $\sim 5.2$  a.u. (513 nm) are due to the temporal overlap between the pump and probe pulses.

Since the VWP motion in the  $B$  state of  $I_2$  is fully understood [5],  $\tau$  will determine the expectation value of  $R$  for the VWP. From this, we obtain the  $R$ -dependent ionization signal of the  $(1,0)$  channel, as shown in Fig. 3. The two different pump wavelengths give almost the same inner  $R_c$ :  $R_c = 7.29 \pm 0.18$  a.u. (513 nm) and  $R_c = 7.28 \pm 0.16$  a.u. (500 nm), and also the same outer  $R_c$  at  $\sim 8.7$  a.u. (within the error bar). The peaks at  $\sim 5.9$  a.u. (500 nm) and  $\sim 5.2$  a.u. (513 nm) are due to the temporal overlap between the pump and probe pulses.

Having established the inner  $R_c$  in the ionization signal of the  $(1,0)$  channel, we need to understand its origin. There are two possibilities: one is from ionization of an inner orbital, and the other is from resonant population transfer from the bound  $I_2^+$  to the  $(1,0)$  channel. However, population transfer would simultaneously increase the  $(1,0)$  signal while decreasing the  $I_2^+$  signal. As this is not seen in Fig. 2, population transfer can be ruled out. Therefore, the inner peak should be associated with ionization of an inner orbital.

The  $B$  state of  $I_2$  has valence orbitals of  $\sigma_g^2 \pi_u^4 \pi_g^3 \sigma_u^1$ . The ionization of the LUMO  $\sigma_u$  electron will leave the molecule in the bound  $I_2^+ X^2 \Pi_{g3/2}$  ( $\sigma_g^2 \pi_u^4 \pi_g^3 \sigma_u^0$ ) state, and this was fully discussed in our previous work [5] in which only one  $R_c$  at  $\sim 8.7$  a.u. was found. On the one hand, the  $(1,0)$  channel must be from the ionization of an inner orbital, HOMO  $\pi_g$ , HOMO  $-1$   $\pi_u$ , or HOMO  $-2$   $\sigma_g$ ; on the other hand, the  $R_c$  implies that the target orbital should show a strong  $R$ -dependent ionization. In this case, the HOMO  $\pi_g$  should be ruled out first, because the final state of  $\sigma_g^2 \pi_u^4 \pi_g^2 \sigma_u^1$  is also bound [21]. The removal of one electron in the HOMO  $-1$   $\pi_u$  orbital could leave the molecule in a dissociating channel. Normally, removal of the HOMO  $-1$  would leave the molecule in the bound  $A$  state, but since the HOMO is excited to the LUMO, the  $\sigma_g^2 \pi_u^3 \pi_g^3 \sigma_u^1$  configuration may not be bound. However, our previous work shows that the HOMO  $-1$   $\pi_u$  orbital does not have a strong  $R$ -dependent

ionization feature [15]. Moreover, it is predicted that  $\pi$  states do not show EI [10]. So the HOMO  $-1 \pi_u$  orbital is also ruled out. Therefore, the  $R_c \sim 7.3$  a.u. must be associated with the HOMO  $-2 \sigma_g$  orbital. In our previous work [15], we did see a strong  $R$ -dependent ionization of the  $\sigma_g$  orbital when the VWP vibrated between 4.4 and 6.2 a.u. in the ground electronic state, and we predicted that there would be an  $R_c$  if the VWP moved to larger  $R$  [15]. Now, we find this  $R_c$ .

In order to determine if this value of  $R_c$  makes physical sense, we note that  $R_c \times I_p$  appears to be a useful way to characterize enhanced ionization, independent of the details of the system under study (see above and [6,9]). Since  $I_p$  of the HOMO  $-2 \sigma_g$  orbital is  $\sim 15.07$  eV (0.554 a.u.) [21,22], we get the product of  $R_c$  and  $I_p$  to be 4.04. The product is different from that of the LUMO  $\sigma_u$  orbital in which  $R_c \times I_p \sim 3$  [5]. The LUMO  $\sigma_u$  orbital has only one active electron, and it is more like a one-electron system with its  $R_c$  well predicted by EL. However, the HOMO  $-2 \sigma_g$  orbital has two equivalent electrons in which the ionic states should play an important role in the ionization. As we do not know of any predictions of this product for enhanced ionization in two-electron systems, we need to answer two questions: is the magnitude of the product similar to that in one-electron systems and do  $R_c$  and  $I_p$  scale inversely?

In order to learn more about  $R_c \times I_p$  in a two-electron system, we consider a one-dimensional model of a generic diatomic molecule  $A_2$  with two equivalent electrons moving in a double-well potential [23,24]:

$$H_s(x_1, x_2, t) = \frac{-Z}{\sqrt{(x_1 - d)^2 + a^2}} + \frac{-Z}{\sqrt{(x_1 + d)^2 + a^2}} \\ + \frac{-Z}{\sqrt{(x_2 - d)^2 + a^2}} + \frac{-Z}{\sqrt{(x_2 + d)^2 + a^2}} \\ + \frac{1}{\sqrt{(x_1 - x_2)^2 + a^2}} - (x_1 + x_2)F(t),$$

where  $Z = 1$  is the charge on each well,  $x_1$  and  $x_2$  are the coordinates of the two electrons,  $R = 2d$  is the internuclear separation,  $a$  is the smoothing parameter of the Coulomb potential, and  $F(t)$  is the electric field strength. Throughout the calculation, atomic units are used.

In this one-dimensional (1D) model, the parameter  $a$  affects the ionization potential  $I_p$ : the smaller the  $a$ , the deeper the ground state.  $a = 0.700$  or  $0.742$  corresponds to  $I_p = 0.90$  or  $0.86$  a.u., respectively. The ionization probability at different  $R$  is obtained after solving the Schrödinger equation. As it turns out (Fig. 4),  $R_c$  becomes smaller as the initial target state becomes more deeply bound. Moreover, this model gives  $R_c \times I_p \sim 3.15$  ( $a = 0.700$ ), and  $R_c \times I_p \sim 3.44$  ( $a = 0.742$ ), verifying the inverse relationship between  $R_c$  and  $I_p$  and showing that the magnitude of this quantity is between 3 and 4, as is true for one-electron systems. Thus, this corroborates our identification of the peak at 7.3 a.u. with enhanced ionization of an inner orbital.

The outer  $R_c$  in the (1,0) channel is at  $\sim 8.7$  a.u., and this is the same as that in the  $I_2^+$  signal since the peaks occur at the same delay. In Ref. [5], we fully studied the EI of the LUMO  $\sigma_u$  state in which the bound  $I_2^+ X^2\Pi_{g3/2}$  state was

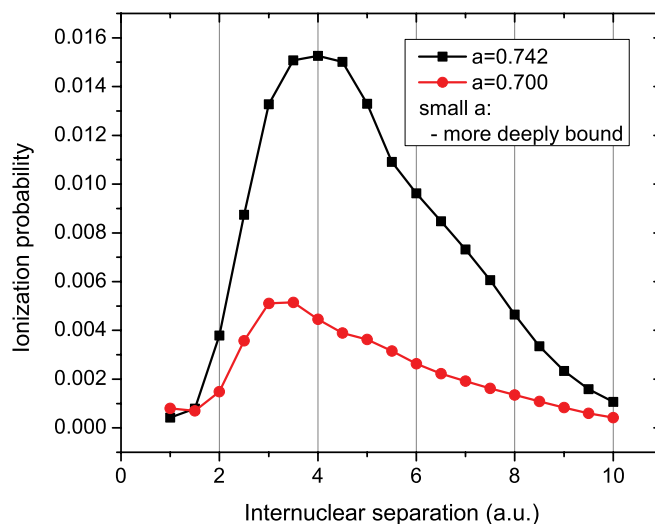


FIG. 4. (Color online) The calculation of the ionization probability as a function of internuclear separation  $R$  with two electrons initially in the ground state. The two different values of  $a$  correspond to different ionization potentials.

the final state and the  $R_c$  was found at  $\sim 8.7$  a.u. The peak at  $\sim 8.7$  a.u. can be considered as a signature of ionizing from the LUMO  $\sigma_u$  state. However, from the molecular orbital picture, the ionization of the LUMO leaves the molecule only in the bound  $I_2^+ X^2\Pi_{g3/2}$  state, not the (1,0) channel. It is a question why the (1,0) channel shows the ionization characteristic of the LUMO  $\sigma_u$  state. One possibility is resonant population transfer between molecular ions. However, population transfer should be weak, if there is any, since the resonant crossing is far away from 8.7 a.u., although this cannot be completely ruled out.

Another possible explanation is the mixture of different molecular orbitals [25] in  $I_2$  when the two I atoms are pulled apart. The molecular orbital picture works well for light molecules, like  $N_2$ ,  $O_2$  [26],  $CO_2$  [27], and  $HCl$  [28]; however, whether it still works properly for heavy molecules, like  $I_2$ , especially when the two atoms are far away from each other, is still an open question. The heavy molecule  $I_2$  shows different ionization characteristics from the light molecules, as seen from the ionization branching ratio of different orbitals. For light molecules, the branching ratio of inner orbitals is usually rather small [28], compared with the HOMO. However, for  $I_2$ , the HOMO  $-2$  provides the dominant single-ionization pathway [15]. At large  $R$ , the  $\sigma_u$  and  $\sigma_g$  orbitals are probably mixed and the electron transfer can occur as the LUMO  $\sigma_u$  electron is ionized. In this case, the ionization feature of the LUMO also appears in the (1,0) channel.

In conclusion, with a pump-probe technique, we generate a VWP in the  $B$  state of  $I_2$  and study the single ionization of the HOMO  $-2 \sigma_g$  orbital. As predicted by previous work, an  $R_c$  is found at  $\sim 7.3$  a.u. This implies that the enhanced ionization also occurs in lower-lying orbitals, not just the HOMO or LUMO. Another  $R_c$  at  $\sim 8.7$  a.u. implies that there might be a mixture of molecular orbitals in  $I_2$  at large  $R$ , since the (1,0) channel shows the ionization feature of the LUMO  $\sigma_u$  orbital.

We would like to acknowledge support from the NSF under Grant No. PHYS-0968799.

- [1] E. Constant, H. Stapelfeldt, and P. B. Corkum, *Phys. Rev. Lett.* **76**, 4140 (1996).
- [2] G. N. Gibson, M. Li, C. Guo, and J. Neira, *Phys. Rev. Lett.* **79**, 2022 (1997).
- [3] Th. Ergler, A. Rudenko, B. Feuerstein, K. Zrost, C. D. Schroter, R. Moshhammer, and J. Ullrich, *Phys. Rev. Lett.* **95**, 093001 (2005).
- [4] D. Pavičić, A. Kiess, T. W. Hansch, and H. Figger, *Phys. Rev. Lett.* **94**, 163002 (2005).
- [5] H. Chen, L. Fang, V. Tagliamonti, and G. N. Gibson, *Phys. Rev. A* **84**, 043427 (2011).
- [6] T. Seideman, M. Yu. Ivanov, and P. B. Corkum, *Phys. Rev. Lett.* **75**, 2819 (1995).
- [7] J. H. Posthumus, L. J. Frasinski, A. J. Giles, and K. Codling, *J. Phys. B* **28**, L349 (1995).
- [8] T. Zuo and A. D. Bandrauk, *Phys. Rev. A* **52**, 2511(R) (1995).
- [9] S. Chelkowski and A. D. Bandrauk, *J. Phys. B* **28**, L723 (1995).
- [10] G. Lagmago Kamta and A. D. Bandrauk, *Phys. Rev. A* **75**, 041401(R) (2007).
- [11] I. Kawata, H. Kono, Y. Fujimura, and A. D. Bandrauk, *Phys. Rev. A* **62**, 031401(R) (2000).
- [12] K. Harumiya, H. Kono, Y. Fujimura, I. Kawata, and A. D. Bandrauk, *Phys. Rev. A* **66**, 043403 (2002).
- [13] E. Dehghanian, A. D. Bandrauk, and G. L. Kamta, *Phys. Rev. A* **81**, 061403(R) (2010).
- [14] A. Saenz, *Phys. Rev. A* **61**, 051402(R) (2000).
- [15] H. Chen, V. Tagliamonti, and G. N. Gibson, *Phys. Rev. Lett.* **109**, 193002 (2012).
- [16] H. Stapelfeldt, E. Constant, and P. B. Corkum, *Phys. Rev. Lett.* **74**, 3780 (1995).
- [17] M. Fushitani, A. Matsuda, and A. Hishikawa, *Opt. Express* **19**, 9600 (2011).
- [18] L. Fang and G. N. Gibson, *Phys. Rev. A* **75**, 063410 (2007).
- [19] L. Fang and G. N. Gibson, *Phys. Rev. A* **81**, 033410 (2010).
- [20] J. Tellinghuisen, *J. Chem. Phys.* **135**, 054301 (2011).
- [21] W. A. de Jong *et al.*, *J. Chem. Phys.* **107**, 9046 (1997).
- [22] R. Mulliken, *J. Chem. Phys.* **55**, 288 (1971).
- [23] G. N. Gibson, *Phys. Rev. A* **67**, 043401 (2003).
- [24] V. Tagliamonti, H. Chen, and G. N. Gibson, *Phys. Rev. A* **84**, 043424 (2011).
- [25] W. Li, A. A. Jaroń-Becker, C. W. Hogle, V. Sharma, X. Zhou, A. Becker, H. C. Kapteyn, and M. M. Murnane, *Proc. Natl. Acad. Sci. USA* **107**, 20219 (2010).
- [26] H. Haken and H. C. Wolf, *Molecular Physics and Elements of Quantum Chemistry* (Springer-Verlag, Berlin, 1994).
- [27] S. Petretti, Y. V. Vanne, A. Saenz, A. Castro, and P. Decleva, *Phys. Rev. Lett.* **104**, 223001 (2010).
- [28] H. Akagi, T. Otobe, A. Staudte, A. Shiner, F. Turner, R. Dörner, D. M. Villeneuve, and P. B. Corkum, *Science* **325**, 1364 (2009).